

# Bismuth in $\text{Ag}_2\text{BiO}_3$ : Tetravalent or Internally Disproportionated?

S. Deibele and M. Jansen<sup>1</sup>*Max-Planck-Institut für Festkörperforschung, Heisenbergstrasse 1, D-70569 Stuttgart*

Received October 29, 1998; in revised form January 28, 1999; accepted January 29, 1999

DEDICATED IN THE MEMORY OF JEAN ROUXEL

**Black, coarse crystalline samples of  $\text{Ag}_2\text{BiO}_3$  have been obtained via solid-state reaction of  $\text{Ag}_2\text{O}$  and  $\text{Bi}_2\text{O}_3$  at an elevated oxygen pressure (250 MPa). The crystal structure determination (*Pnna*;  $a = 597.5(1)$ ,  $b = 631.1(1)$ ,  $c = 956.3(2)$  pm;  $Z = 4$ ; 749 independent reflections,  $R1 = 0.043\%$ ,  $wR2 = 0.098\%$ ) reveals a three-dimensional framework of distorted, edge- and corner-sharing Bi–O octahedra. Silver is in a linear twofold, and in an approximately trigonal planar coordination. The cation partial structure  $\text{Ag}_2\text{Bi}$  has the same topology as the cubic Laves phase  $\text{Cu}_2\text{Mg}$ . All bismuth atoms occupy the same crystallographic site and are structurally indistinguishable. Thus, the crystallographic features and composition suggest the presence of tetravalent bismuth. However, this is not compatible with the physical properties ( $\text{Ag}_2\text{BiO}_3$  is semiconducting and diamagnetic) observed, and some kind of charge ordering must be assumed. The structural response is weak and not noticeable but in a slight anomaly of one of the thermal displacement parameters.** © 1999 Academic Press

## INTRODUCTION

Valence states of bismuth higher than +III, especially the intermediate tetravalent state, deserve particular attention because of the crucial role they seem to play in the superconductors  $\text{BaPb}_{1-x}\text{Bi}_x\text{O}_3$  (1) and  $\text{Ba}_{1-x}\text{K}_x\text{BiO}_3$  (2), which are the only copper-free oxidic HTSC's known until now. The stability of the pentavalent state decreases from arsenic to bismuth; this becomes obvious when comparing the conditions at which, e.g., the binary pentaoxides form:  $\text{As}_2\text{O}_5$  (3, 4) can be synthesized at ambient pressure, whereas during the preparation of  $\text{Sb}_2\text{O}_5$  (5, 6) an elevated oxygen pressure must be maintained, and up to now, pure  $\text{Bi}_2\text{O}_5$  has not been obtained at all. Instead, most attempts to synthesize binary or multinary bismuth(V) oxides have only lead to incompletely oxidized phases. Thermal dehydration of  $\text{HBiO}_3 \cdot n\text{H}_2\text{O}$  in a steel autoclave at  $p(\text{O}_2) \geq 250$  MPa yielded the mixed-valent binary oxide  $\text{Bi}_4\text{O}_7$  (7). X-ray powder diffractometry is lending some evidence that  $\text{Bi}_4\text{O}_7$

represents a charge-ordered triclinic variant of the pyrochlore type of structure, mainly because it is isostructural to  $\text{Bi}_3^{+III}\text{Sb}^{+V}\text{O}_7$  (7). Unambiguous evidence for the presence of well-defined  $\text{Bi}^{+V}$  and  $\text{Bi}^{+III}$  sites in the same compound has been obtained by a single-crystal structure determination on  $\text{Ag}_{25}\text{Bi}_3\text{O}_{18} \equiv \text{Ag}_{25}\text{Bi}_2^{+III}\text{Bi}^{+V}\text{O}_{18}$ .  $\text{Bi}^{+V}$  is coordinated by six oxygen atoms at a distance of 213 pm, while  $\text{Bi}^{+III}$  has three nearest neighbors at 221 pm (8, 9).

However, in most cases, the valence state of bismuth in oxidized phases is not easily assigned. Examples can be found among the wide variety of bismuth dioxides (10). In particular, the controversy regarding  $\text{BaBiO}_3$ , whether it is a bismuthate(IV) or a Bi(III/V) mixed-valent phase with two distinguishable bismuth sites, is an impressive example for this. First reports on  $\text{BaBiO}_3$  state that it exhibits the perovskite type of structure (11, 12, 13). Neutron diffraction studies (14) resulted in monoclinic unit cell containing four formula units. The important feature of this latter structure model is that bismuth atoms occupy two crystallographically independent sites with different average interatomic distances  $\text{Bi}(1)\text{--O} = 228.3$  pm and  $\text{Bi}(2)\text{--O} = 212.6$  pm, respectively. These inequivalent Bi sites have been attributed to a charge-ordering phenomenon, suggesting the mixed-valent formulation  $\text{Ba}_2\text{Bi}^{+III}\text{Bi}^{+V}\text{O}_6$ . However, other authors have pointed out that the Bi–O bond lengths, as found for the two sites, do not differ sufficiently to justify such rigid assignment. Therefore, a partial charge transfer among the different bismuth sites is conceivable (15, 16). This unique situation seems to be matched rather closely by the novel silver bismuthate  $\text{Ag}_2\text{BiO}_3$  presented here. So far,  $\text{Ag}_4\text{Bi}_2\text{O}_5$  (17),  $\text{Ag}_3\text{BiO}_3$  (18),  $\text{Ag}_5\text{BiO}_4$  (18), and  $\text{Ag}_{25}\text{Bi}_3\text{O}_{18}$  (8, 9) have been shown to exist in the system  $\text{Ag}_2\text{O}/\text{BiO}_x$ .

## EXPERIMENTAL

### Synthesis

$\text{Ag}_2\text{BiO}_3$  was prepared by solid-state reaction of the binary oxides by applying an elevated oxygen pressure. As

<sup>1</sup>To whom correspondence should be addressed.



starting materials, reactive Ag<sub>2</sub>O precipitated from an acidic AgNO<sub>3</sub> solution and Bi<sub>2</sub>O<sub>3</sub> (Riedel-de Haen, 99%) have been used. By X-ray powder diffraction, the educts were proven to be single phase. Ag<sub>2</sub>O and Bi<sub>2</sub>O<sub>3</sub> were mixed in the molar ratio of 2:1 and then annealed for 3–5 days in gold crucibles placed in stainless-steel autoclaves (19) (ATS 351, modified Bridgeman seal,  $V = 20 \text{ cm}^3$ ). The optimized reaction temperature and oxygen pressure are 250°C and 250 MPa, respectively. Two milliliters of a 5 M KOH solution was added as an accelerator. At oxygen pressures below 250 MPa the reacted samples contain Ag<sub>4</sub>Bi<sub>2</sub>O<sub>5</sub> as a byproduct.

### Structure Determination

For data collection, a rod-shaped single crystal of Ag<sub>2</sub>BiO<sub>3</sub> was mounted on a four circle diffractometer (CAD4, Enraf Nonius, Delft, Netherlands; MoK $\alpha$  radiation, graphite monochromator,  $\lambda = 71.073 \text{ pm}$ ). Essential crystal data and experimental details of the structure determination are listed in Table 1<sup>2</sup>. For checking the correctness of the space group and the absence of weak superstructure reflexes, long exposed Weissenberg photographs were made. These investigations confirm the results of the diffractometer data.

Data reduction was carried out with the program CADSHEL (20), and an absorption correction ( $\Psi$  scans, HABITUS (21)) was applied. The structure was solved by the Patterson technique (SHELXS-86 (22)) and refined by full-matrix least-squares methods (SHELX-93 (23)). Structure plots were generated using the program KPLOT (24).

The unit-cell dimensions used in all calculations were determined by X-ray powder diffraction (STOE-Stadi P diffractometer, germanium monochromator, CuK $\alpha$  radiation,  $\lambda = 154, 056 \text{ pm}$ , Si as an external standard).

### Chemical Analyses

The cation ratio in Ag<sub>2</sub>BiO<sub>3</sub> was determined by energy dispersive X-ray analysis on several crystals (Zeiss DMS 940, EDAX PV9800). The EDX spectra were recorded at an acceleration energy of 25 keV, and the Ag and Bi L-lines were used to calculate the cation concentrations.

### Thermal Analyses

The thermal behavior was investigated by DTA and TGA (STA 429, Netzsch, Selb, Germany); the decomposition products were characterized by X-ray powder diffraction.

<sup>2</sup>Further details of the structure determination have been deposited as supplementary publication No. CSD-410665 for Ag<sub>2</sub>BiO<sub>3</sub>. Copies may be obtained from the Fachinformationszentrum Karlsruhe, D-76344 Eggenstein-Leopoldshafen, Germany.

**TABLE 1**  
**Crystal Data and Structure Refinement for Ag<sub>2</sub>BiO<sub>3</sub>**

Formula	Ag <sub>2</sub> BiO <sub>3</sub>
Formula weight	472.72 g/mol
Space group	<i>Pnna</i> (No. 52)
Unit cell dimensions (from powder data)	$a = 597.5(1) \text{ pm}$ $b = 631.1(1) \text{ pm}$ $c = 956.3(2) \text{ pm}$
Cell volume	$360.6(2) \times 10^6 \text{ pm}^3$
Z	4
Calculated density	8.693 g/cm <sup>3</sup>
Wavelength	MoK $\alpha$
Scan	$\omega/\theta$
Theta range for data collection	0–35°
<i>hkl</i> (min/max)	$-2 < h < 9$ $0 < k < 10$ $-15 < l < 15$
Number of reflections measured	1386
Number of unique reflections	749
Number of parameters	32
Absorption coefficient	59.253 mm <sup>-1</sup>
Corrections	Lorentz-polarization, absorption
$R_{\text{int}}^a$	0.028
$R1^b$ (all data)	0.043
$wR2^c$ (all data)	0.098

$$^a R_{\text{int}} = \sum |F_0^2 - F_0^2(\text{mean})| / \sum [F_0^2]$$

$$^b R1 = \sum ||F_0| - |F_c|| / \sum |F_0|$$

$$^c wR2 = (\sum [w(F_0^2 - F_c^2)^2] / \sum [w(F_0^2)^2])^{1/2}$$

### Physical Properties

The magnetization was recorded using a Squid magnetometer (Quantum Design MPMS; 5–300 K). Measurements of the electrical conductivity of Ag<sub>2</sub>BiO<sub>3</sub> were performed with an impedance analyzer (Hewlett-Packard HP 41924) on pressed pellets (diameter: 6 mm; thickness: 1 mm).

## RESULTS

By solid-state reaction between Ag<sub>2</sub>O and Bi<sub>2</sub>O<sub>3</sub>, Ag<sub>2</sub>BiO<sub>3</sub> has been prepared for the first time. The black crystals are stable in air and moisture. Ag<sub>2</sub>BiO<sub>3</sub> decomposes at 477°C in one step to Bi<sub>2</sub>O<sub>3</sub> and elemental silver. The weight loss, as determined by TG (5.1 wt%), agrees well with the calculated value (5.2 wt%), assuming that Ag<sub>2</sub>BiO<sub>3</sub> transforms to Bi<sub>2</sub>O<sub>3</sub> and Ag by release of oxygen. According to EDX analyses (average of 25 spots), the Ag/Bi ratio is 1.93:1 and the samples are free of potassium (detectability limit with EDX: 0.3%).

The results of the X-ray crystal structure determination, such as atomic parameters, thermal parameters, and interatomic distances, are documented in Tables 2–4, respectively. Measurements of the magnetic susceptibility show a virtually temperature independent diamagnetic behavior. In the temperature range investigated, –100 to 300°C, Ag<sub>2</sub>BiO<sub>3</sub> is semiconducting with a band gap of 0.7 eV.

**TABLE 2**  
Positional and Isotropic Displacement ( $U_{eq}$ )<sup>a</sup> Parameters  
for Ag<sub>2</sub>BiO<sub>3</sub>

Atom	x	y	z	$U_{eq}$ [pm <sup>2</sup> × 10 <sup>-1</sup> ]
Bi(1)	0.25	0	0.1042(1)	11(1)
Ag(1)	0	0	0.5	26(1)
Ag(2)	0.7758(2)	0.25	0.25	27(1)
O(1)	0.5669(17)	0.1796(14)	0.0603(10)	17(2)
O(2)	0.1430(27)	0.25	0.25	54(7)

$${}^a U_{eq} = 1/3(U_{11} + U_{22} + U_{33}).$$

### DISCUSSION

The crystal structure of Ag<sub>2</sub>BiO<sub>3</sub> contains one crystallographically independent site for bismuth, which is in a distorted octahedral coordination by oxygen. While the Bi–O bond lengths cover the relatively small range from 220.1 to 224.6 pm, some of the O–Bi–O angles deviate considerably by up to 20° from the ideal values. These features can be traced back to the way in which the BiO<sub>6</sub> units are interconnected to form a three-dimensional framework. Each oxygen atom within the Bi–O partial structure connects two bismuth atoms, which should lead to bonds of comparable lengths, in agreement with the experimental data. The BiO<sub>6</sub> octahedra are linked via common edges and vertices. Bridging via *cis*-oriented edges leads to zigzag chains which run along [100]. These chains are connected three-dimensionally by edge sharing through the remaining two oxygen atoms at each octahedron, c.f. Fig. 1. It is well-known for crystal chemical patterns that edges shared by polyhedra are generally shortened significantly. Thus, this can be seen as the main reason for the mentioned angular distortions of the BiO<sub>6</sub> octahedra. The two independent Ag(1) and Ag(2) are in a linear and trigonal planar coordination, respectively.

This new ternary silveroxide shows a structural feature that seems to be common to all silver-rich oxides (25). In spite of their positive charges, the silver cations develop

**TABLE 3**  
Anisotropic Displacement Parameters<sup>a</sup> for Ag<sub>2</sub>BiO<sub>3</sub>  
(pm<sup>2</sup> × 10<sup>-1</sup>)

Atom	$U_{11}$	$U_{22}$	$U_{33}$	$U_{23}$	$U_{13}$	$U_{12}$
Bi(1)	15(1)	10(1)	9(1)	0	0	1(1)
Ag(1)	25(1)	12(1)	40(1)	0(1)	−6(1)	−1(1)
Ag(2)	25(1)	34(1)	20(1)	−8(1)	0	0
O(1)	26(4)	13(4)	12(4)	−4(3)	−2(3)	−2(3)
O(2)	29(7)	113(20)	19(7)	−37(12)	0	0

<sup>a</sup>The anisotropic displacement factor exponent takes the form

$$-2\pi^2[U_{11}h^2a^{*2} + \dots + 2U_{12}hka^*b^*].$$

**TABLE 4**  
Selected Bond Lengths (pm) and Angles (°) for Ag<sub>2</sub>BiO<sub>3</sub>

Bi(1)–O(1)	224.6(10)	2 ×	O(1)–Bi(1)–O(1')	90.1(5)
Bi(1)–O(1')	222.6(9)	2 ×	O(1)–Bi(1)–O(1'')	91.5(3)
Bi(1)–O(2)	220.1(5)	2 ×	O(1')–Bi(1)–O(1'')	73.2(4)
Ag(1)–Ag(1')	298.8(1)	2 ×	O(1')–Bi(1)–O(1''')	158.5(5)
Ag(1)–Ag(2)	316.2(1)	2 ×	O(2)–Bi(1)–O(2')	101.3(2)
Ag(1)–Ag(2')	330.5(1)	2 ×	O(2)–Bi(1)–O(1)	162.9(4)
Ag(2)–Ag(2)	317.1(1)	2 ×	O(2')–Bi(1)–O(1)	86.6(3)
Ag(1)–O(1)	214.0(9)	2 ×	O(2)–Bi(1)–O(1')	103.6(5)
Ag(2)–O(1)	224.6(9)	2 ×	O(2')–Bi(1)–O(1')	90.1(4)
Ag(2)–O(2)	219.0(20)		O(1)–Ag(1)–O(1')	180.0
Bi(1)–Bi(1)	359.1(1)	2 ×	O(1)–Ag(2)–O(1')	112.5(5)
			O(2)–Ag(2)–O(1)	123.8(3)
			O(2)–Ag(2)–O(1')	123.8(3)

close contacts with distances as short, and sometimes even shorter, as those in metallic silver. Considering all Ag–Ag separations up to the van der Waals distance (340 pm) as typical topologies sections of the fcc structure of elemental silver are frequently found. In the case of Ag<sub>2</sub>BiO<sub>3</sub>, the silver atoms are arranged to tetrahedra, which are interconnected via all four vertices. This network corresponds to the copper partial structure of the Laves phase MgCu<sub>2</sub>. As the bismuth positions in relation to the Ag partial structure correspond to the magnesium positions in MgCu<sub>2</sub>, the cation partial structure of Ag<sub>2</sub>BiO<sub>3</sub> is topologically equivalent to the Laves type of structure. Thus, the approach of describing crystal structures by starting from the cations (26, 27) applies pretty well to Ag<sub>2</sub>BiO<sub>3</sub>.

The composition of the title compound, as determined by single-crystal X-ray structure analysis and confirmed by EDX- as well as by TG-analysis, implies a formal tetravalent state of bismuth. This interpretation seems to be conclusive from the structural point of view, as the Bi–O lengths are intermediate between Bi<sup>+III</sup>–O and Bi<sup>+V</sup>–O distances, and as there is only one crystallographic site occupied by bismuth. Furthermore, there are pronounced structural similarities with Ag<sub>2</sub>TiO<sub>3</sub> (28), which clearly contains tetravalent titanium. The presence of true tetravalent bismuth should give rise to Curie paramagnetism or metallic behavior, depending on the 6s electron being localized or delocalized. However, magnetic and conductivity measurements are not compatible to either one of these assumptions. A band gap of 0.7 eV, and diamagnetic behavior strongly suggest pairwise ordering of the residual valence electrons, or by taking into account the collective character of the phenomena under discussion, splitting of the half occupied 6s band through a Peierls type distortion. As already mentioned, the structural features do not lend any support to an internal disproportion corresponding to 2Bi<sup>+IV</sup> = Bi<sup>+III</sup> + Bi<sup>+V</sup>. However, the displacement parameter  $U_{22}$  of the O(2) atom, which defines the common

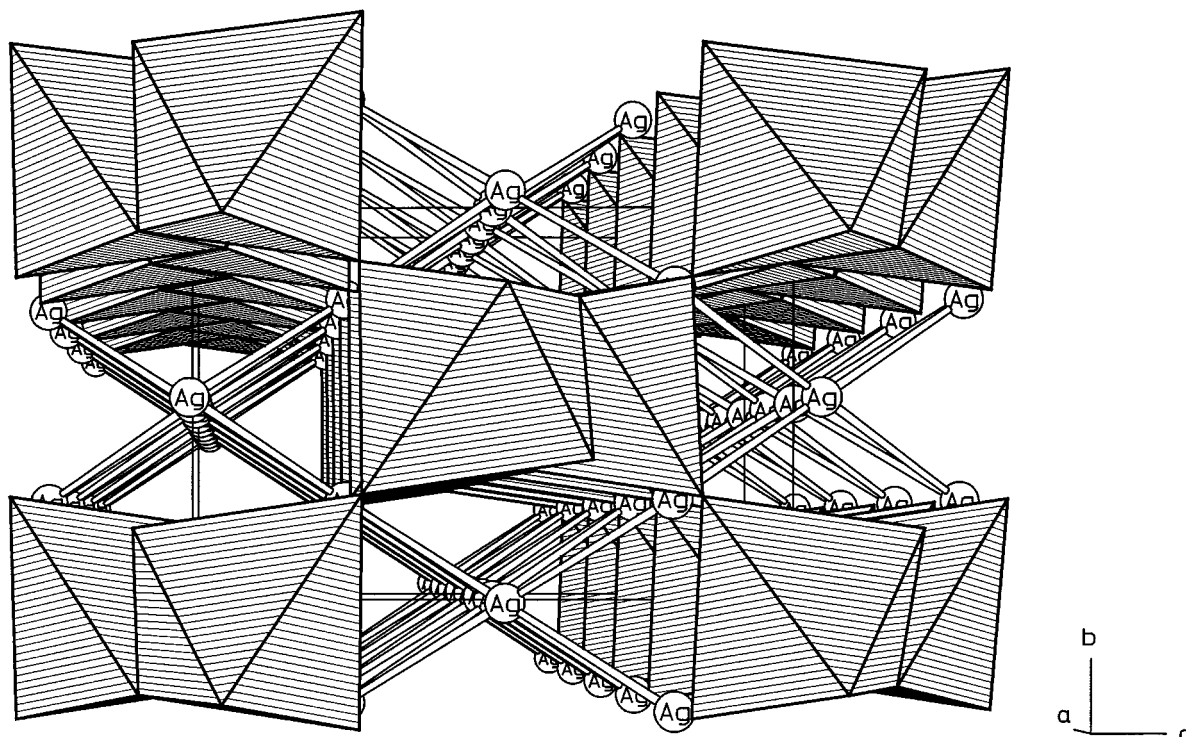


FIG. 1. Perspective view of the crystal structure of  $\text{Ag}_2\text{BiO}_3$ ;  $\text{BiO}_6$  is shown as a hatched octahedra, and Ag-Ag contacts ( $< 340$  pm) are shown as rods.

edges within the chains of octahedra, is marginally, but significantly, enlarged compared to all the other anisotropic temperature parameters. This slight structural anomaly appears to be intrinsic, since it was found in refinements we have performed on independent data sets from different

crystals. An attempt to refine twinning model has failed, probably because the contribution of O(2) to the scattering power is too low, and the deviation from the average structure is too small. Refinement of O(2) as a split atom was convergent. However, this did not result in improved  $R$  values or lower residual electron densities in the difference fourier map. Although the split atom model allows one to assign alternating shorter and longer Bi-O(2) distances, the remaining Bi-O bond lengths do not follow this tendency.

## CONCLUSION

All experimental findings available to date are in agreement with the assumption of charge ordering, or an at least partial internal disproportionation, at the bismuth sites in  $\text{Ag}_2\text{BiO}_3$ . This Peierls type of distortion leads to a splitting of the half-filled 6s band, explaining the observed magnetic properties and electrical conductivity. The structural response has not yet been understood in detail; however, the magnitude of the displacements involved can be estimated to be no longer than 10–30 pm.

## ACKNOWLEDGMENT

Support by the Fonds der Chemischen Industrie is gratefully acknowledged.

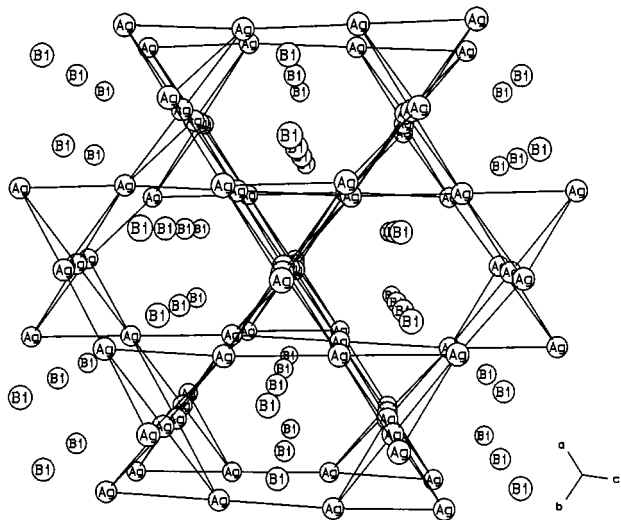


FIG. 2. The cation partial structure of  $\text{Ag}_2\text{BiO}_3$ .

## REFERENCES

1. A. W. Sleight, J. L. Gillson, and P. E. Bierstedt, *Solid State Commun.* **17**, 27 (1975).
2. R. J. Cava, B. Batlogg, J. J. Krajewski, R. C. Farrow, L. W. Rupp Jr., A. E. White, K. T. Short, W. F. Peck, and T. Y. Kometani, *Nature* **332**, 814 (1988).
3. M. Jansen, *Angew. Chem.* **89**, 326 (1977); *Angew. Chem., Int. Ed. Engl.*, **16**, 315 (1977).
4. M. Jansen, *Z. Anorg. allg. Chem.* **441**, 5 (1978).
5. M. Jansen, *Acta Crystallogr., Sect. B* **35**, 539 (1979).
6. E. Schwarzmann, H. Rumpel, and W. Berndt, *Z. Naturforsch. B* **32**, 617 (1977).
7. J. Begemann and M. Jansen, *J. Less-Common Met.* **156**, 123 (1989).
8. M. Bortz and M. Jansen, *Angew. Chem.* **103**, 841 (1991); *Angew. Chem., Int. Ed. Engl.* **30**, 883 (1991).
9. M. Bortz and M. Jansen, *Z. Anorg. Allg. Chem.* **612**, 113 (1992).
10. "Gmelins Handbuch der anorg. Chemie, Bismut-Ergänzungsband, 8," P. 642. Auflage, 1964.
11. R. Scholder, K. Ganter, H. Glaser, and G. Merz, *Z. Anorg. Allg. Chem.* **319**, 375 (1963).
12. Yu. N. Venetsev, *Mater. Res. Bull.* **11**, 1085 (1971).
13. J. Th. W. De Hair and G. Blasse, *Solid State Commun.* **12**, 727, (1973).
14. D. E. Cox and A. W. Sleight, *Solid State Commun.* **19**, 969 (1976).
15. L. F. Mattheis and D. R. Hamann, *Phys. Rev. B* **28**, 4227 (1983).
16. C. Chaillout and J. P. Remeika, *Solid State Commun.* **56**, 829 (1985).
17. M. Jansen and S. Deibele, *Z. Anorg. Allg. Chem.* **622**, 539 (1996).
18. M. Bortz and M. Jansen, *Z. Anorg. Allg. Chem.* **619**, 1446 (1992).
19. C. Linke and M. Jansen, *Z. Anorg. Allg. Chem.* **623**, 1441 (1997).
20. J. Kopf, "CADSHEL V 3.10." University of Hamburg, Germany, 1996.
21. W. Herrendorf and H. Bärnighausen, "HABITUS." University of Karlsruhe, Germany, 1993.
22. G. Sheldrick, "SHELXS-86." University of Göttingen, Germany, 1986.
23. G. Sheldrick, "SHELXL-93." University of Göttingen, Germany, 1993.
24. R. Hundt, "KLOT." University of Bonn, Germany, 1985-1997.
25. M. Jansen, *Angew. Chem.* **99**, 1136 (1987); *Angew. Chem. Int. Ed. Engl.* **26**, 1098 (1987).
26. M. O'Keeffe and B. G. Hyde, "Structure and Bonding," Vol. 61. Springer-Verlag, Berlin, Heidelberg, 1985.
27. A. Vegas and R. Isea, *J. Solid State Chem.* **131**, 358 (1997).
28. C. Linke and M. Jansen, *J. Solid State Chem.* **134**, 17 (1997).